



ANALYSIS OF RECORDS OF THE 1999 CHICHI EARTHQUAKE IN TAIWAN AND CORRELATION WITH HOUSING DAMAGE

Takanobu SUZUKI¹

SUMMARY

Real-time disaster prevention technology based on actual earthquake motion is potentially useful for reducing damage, and appropriate information obtained from seismometers can be used as a damage index. Using the data of the 1999 Chichi Earthquake, this study compares the housing damage with the ground motion in central Taiwan. The results represent new knowledge showing that a specific wave with long-period pulse caused extensive housing damage due to severe ground motion. The method proposed in this paper can be used to analyze earthquake records in order to characterize the earthquake damage distribution.

INTRODUCTION

Real-time disaster prevention technology based on actual earthquake motion is potentially useful for reducing damage, and appropriate information obtained from seismometers can be used as a damage index. The 1999 Chichi Earthquake in Taiwan was a large-scale reverse fault movement that resulted in severe earthquake motion and extensive housing damage or others (1). Seismic records of the event were captured at observation points distributed throughout the Taiwan mainland, and Central Weather Bureau of Taiwan (CWB) has made these records available to the public (2). Using this data, this study compares the housing damage with the ground motion in central Taiwan. The results represent new knowledge showing that a specific wave with long-period pulse caused extensive housing damage due to severe ground motion. The group including author proposed the detection method for liquefaction comparing some index values with the criterion (3). The features learned from the Chichi earthquake, is available for a future earthquake with a reverse fault.

It was not easy to integrate the specific wave with long-period pulse into the displacement waveform. Removal of a drift component responsible for dispersion in the data allowed the permanent displacement to be calculated by trapezoidal integration. After the special treatment, the results are consistent with official reports of ground displacement, indicating that the method proposed in this paper can be used to analyzed earthquake records in order to characterize the earthquake damage distribution.

¹ Toyo University, Faculty of Engineering, Japan, Email: suzuki@eng.toyo.ac.jp

Table 1 List of housing damage (unit: percentage)

District Name	Complete Collapse	Partial Collapse	Total
Sanyi	0	0.05	0.05
Juolan	9.9	6.8	16.7
Shrgang	47.6	30.1	77.7
Dungshr	33.6	35.6	69.2
Shinshe	22.1	16.4	38.5
Fengyuan	3.6	1.4	5.0
Taichun(whole)	0.9	1.3	2.2
Jung qu	0.04	0.33	0.4
Dung qu	0.16	1.89	2.05
Shi qu	0.04	0.13	0.17
Nan qu	2.9	7.4	10.3
Bei qu	2.5	0.9	3.3
Shituen qu	0.0	0.2	0.2
Nantuen qu	0.0	0.5	0.5
Beituen qu	1.1	0.6	1.6
Taiping	4.7	3.8	8.5
Dali	5.5	8.8	14.3
Wufeng	16.9	14.6	31.5
Tsutuen	9.7	15.2	24.9
Nantou	17.6	21.4	39.0
Mingjian	3.3	4.1	7.4
Juahan	16.4	18.0	34.4
Gukeng	2.1	4.0	6.0
Jungliao	51.2	28.7	79.9
Jiji	47.8	22.0	69.8
Shueili	8.7	17.8	26.5
Yuchr	46.0	28.6	74.5
Puli	24.7	26.3	51.0

HOUSING DAMAGE

The Chichi earthquake produced strong ground motion and fault displacement, resulting in extensive housing damage. Publicly available housing damage data collected by the Taiwanese government details the damage in 6 counties and cities in central Taiwan, including Miaoli County, Taichung County, Taichung City, Nantou County, Yunlin County, and Changhus County (4). The damage ratios for complete collapse (demolished) and partial collapse (repairable) have been calculated for each xiang, chen or city. Table 1 shows the housing damage ratios for representative districts of the 6 areas for which data is available. Taichung City, which is the largest city in the area, lies in a basin bordered by tablelands to the west and the Taiwan mountains to the east. The zone of severe damage lies along the fault line in a valley, as well as along the foot of the mountain and basin.

The results of the damage ratio analysis are shown in Figure 1. The districts examined extend from Sanyi to Gukeng on the fault line (north to south), and from Jungliao to Puli in the mountains near the epicenter. The ratio for Taichung City is the average of the entire city. The districts with the highest damage ratios

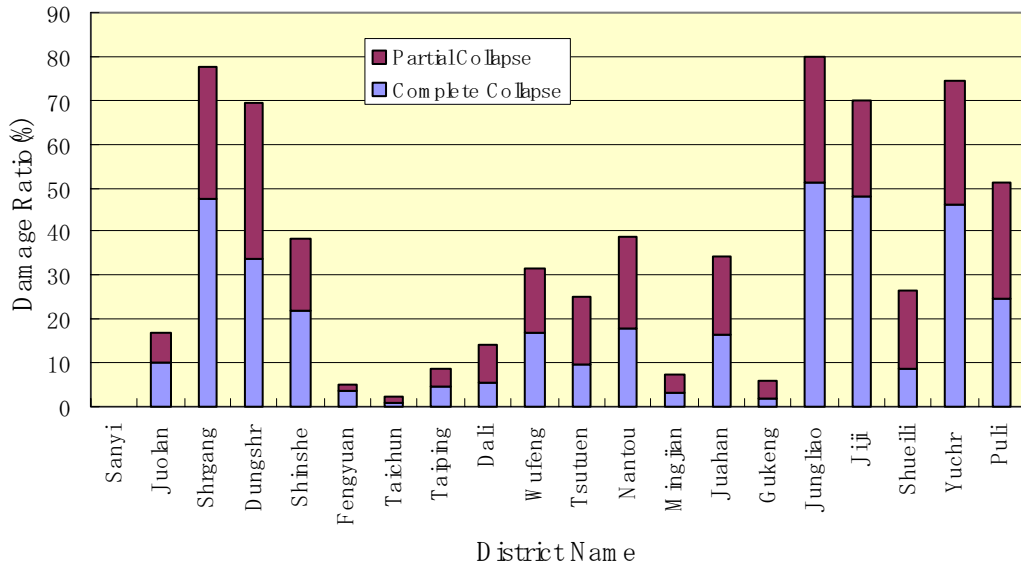


Figure1 Damage ratios of focused region

were Shrgang, Dungshr, Jungliau, Chichi, Yuchr, and Puli, all exceeding 50% partial collapse. The complete collapse rate and partial collapse rate are almost proportional. Shrgang and Dungshr are located on the northern part of the fault, and both have high damage ratios. Jungliau, Chichi, Yuchr, and Puli are located near the epicenter in the Taiwan mountains. The damage ratio in other districts, Wufeng, Tasutuen, and Nantou, varied from 10% to 40% for areas within the fault zone. The ratio for Mingjian, located on the south of the fault line over Gukeng, varies from 10% to 30%. Taichung City consists of a number of wards, including Dung-qu, Nan-qu, Bei-qu, and Beituen-qu, which although lying relatively close to the fault, have only a 10% damage ratio.

GROUND MOTION

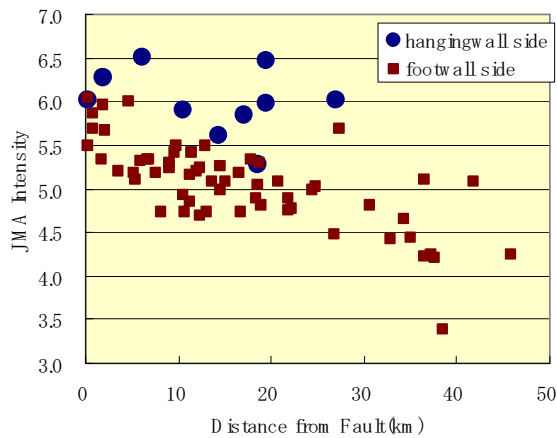
In Taiwan, the Central Weather Bureau Seismic Network (CWBSN), a strong-motion monitoring network, has been deployed by the central meteorological office. Data from these seismographs is transmitted to the head office of the CWB in Taipei by a telemetry system, and the focal region is determined by computer within about 1 min. The observation points are installed at intervals of approximately 3 km in urban areas on free ground. The data from each observation point is compared here with the average damage ratio of the relevant district, taking the average earthquake motion when multiple observation points lie in the same district. Table 2 lists the calculated motion for the main districts. The peak ground acceleration (PGA) was highest at Wufeng, Minjiang, and Gukeng along the southern part of the Charunpu fault, whereas the peak ground velocity (PGV) was largest at Shrgang, Beitun-qu, Wufeng, Tasutuen, and other observation points near the fault, in some cases exceeding 1 m/s. The largest PGV values were generated in areas exhibiting peak ground displacement (PGD) of more than 1 m, which includes permanent displacement. The method of calculation is described later. The calculated zero cross time in central Taiwan are significantly larger for previous earthquakes, with the largest being 3.1 s at Shrgang. Many records exceed 1 s. It is considered that the long zero cross time also results in large displacement of the ground.

Table2 Calculated ground motion of the representative districts

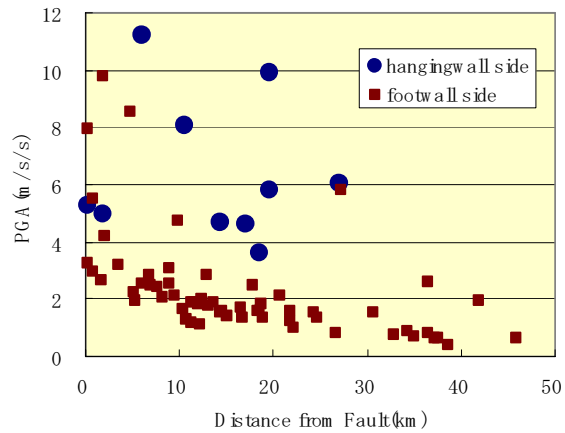
D istrict N am e	JM A I ntensity	PGA (m/s/s)	PGV (m/s)	PGD (m)	SI (m/s)	Tz (sec)	Horizontal P em anent D isplacem ent (m)	Vertical P em anent D isplacem ent (m)
Shrgang	6.0	5.30	2.91	8.61	0.83	3.1	8.40	3.44
Fengyuan	5.7	2.98	0.88	1.61	0.62	1.6	0.93	- 0.02
Taichun								
Shi qu	5.1	2.05	0.46	1.15	0.27	1.7	0.53	- 0.07
Nan qu	5.3	2.86	0.55	6.91	0.38	1.4	-	-
Bei qu	5.2	2.26	0.48	1.27	0.35	1.8	0.56	- 0.12
Shituen qu	4.8	1.42	0.47	0.97	0.21	2.3	0.40	0.00
Beituen qu	5.6	3.48	1.08	3.40	0.66	2.0	3.28	1.05
Dali	5.9	5.50	0.98	1.88	0.86	1.7	1.38	- 0.20
Wufeng	6.1	7.94	1.32	2.48	0.85	1.4	2.97	- 0.07
Tsutuen	5.5	3.25	1.16	1.71	0.44	1.0	1.18	0.00
Nantou	5.7	4.20	0.71	0.80	0.59		0.35	-
Mingjian	6.0	9.83	0.68	1.28	0.64	1.2	0.59	0.00
Gukeng	5.9	6.85	0.85	0.52	0.95	1.3	0.34	- 0.08
Shueili	5.6	4.71	0.44	1.32	0.49	0.7	1.62	- 0.01
Yuchr	5.9	6.45	0.76	2.00	0.92	0.9	2.17	0.14
Puli	6.0	6.06	0.70	1.98	0.90	0.7	1.93	- 0.46

The calculated points in central Taiwan are within 50 km of the fault. Figure 2 shows the relationship between the characteristic value of ground motion and distance from the fault, with the data distinguished between the hanging wall side and the footwall side. Figure 2(a) shows the attenuation of Japan Meteorological Agency (JMA) seismic intensity. The values are distributed between 4 and 6 in this 50 km radius, and the values on the hanging wall side are larger than the values on the foot wall side. There is no tendency for the seismic intensity to peak remarkably near the fault itself. Figure 2(b) shows the maximum acceleration synthesized from the two horizontal components. The acceleration varies from 3 m/s/s to about 10 m/s/s in the fault vicinity, with highest accelerations observed in the mountains and near the southern tip of the Charunpu fault closest to the hypocenter. The values on the hanging wall side are larger similarly to JMA intensity. Figure 2(c) shows a plot of the maximum root mean square (RMS) velocity synthesized from the NS and EW directions. The values for TCU068 (Shrgang) and TCU052 (Beituen qu), which are located in the fault vicinity on the hanging wall side, exceed 2 m/s. The plots are uniform (~0.5 m/s) within 30 km of the fault. Figure 2(d) shows the maximum zero cross time. Many values exceed 1 s. Except for 2 values (TCU068 and TCU052), the values on the foot wall side are larger than the values on the hanging wall side, and it is considered that the long zero cross time is generated from surface waves or fault movement.

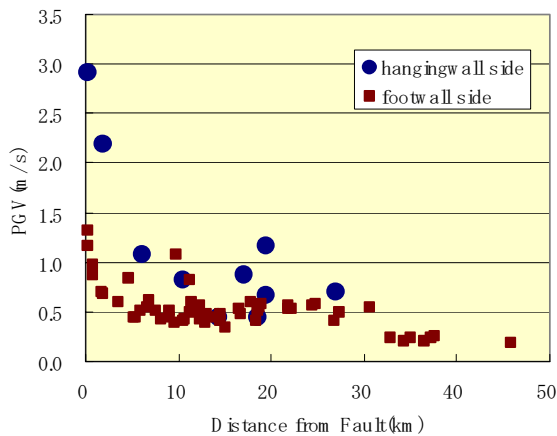
The spectral intensity (SI) value is used to be in good agreement with the PGV according to a normal regression, also be in good agreement with seismic intensity. Tong and Yamazaki proposed some regression equations on it (5). The SI value calculated using same data is compared with the PGV. Figure 3 shows the relationship between PGV and SI Value. As above mentioned, PGV is largest in the vicinity of the fault. However, the SI values (~1 m/s) are much smaller than the PGV values (~4 m/s). It is considered that the component with period longer than 2.5 s is eliminated in the calculation of SI Value



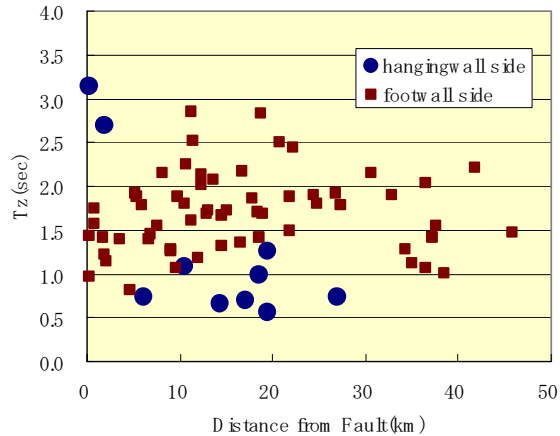
(a) JMA Intensity



(b) Peak ground acceleration



(c) Peak ground velocity



(d) Maximum zero cross time

Figure 2 Relationship between the characteristic value of ground motion and distance from the fault

due to a low-cut filtering effect. In the case of the earthquake with reverse fault movement, the SI value is not in good agreement with the PGV value.

COMPARISON

The housing damage is compared with the ground motion in central Taiwan area in this section. Figure 4 shows plots of the housing collapse rates against the characteristic values of earthquake ground motion in each district. Figure 4(a) shows the results for measured seismic intensity. Collapse begins at a seismic intensity of 5 to 5.5, and the rate increases exponentially. Only one point stands out from the others, corresponding to TCU068 in Shrgang village. The data for this site stands out in all of the plots. The reason is that the ground motion of the severely damaged districts, such as Dungshr, Jungliaw and Chichi, is uncertain. Figure 4(b) shows the relationship between the damage ratio and the calculated SI value. No clear trend can be seen in the graph, because the damage ratio changes with 10% from 80% in the level over 0.8 m/s. Especially, the most right hand plot is Gukeng, at which the damage ratio is 6%. Figure 4(c) shows the relationship between the damage ratio and PGV. In addition to the plot for Shrgang, Beituen-qu in Taichung City stands out, with a PGV of 1.07 m/s but small damage ratio.

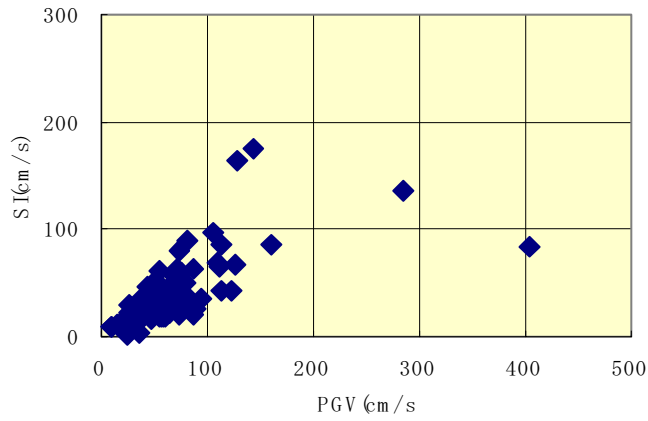


Figure3 Comparison between PGV and SI value

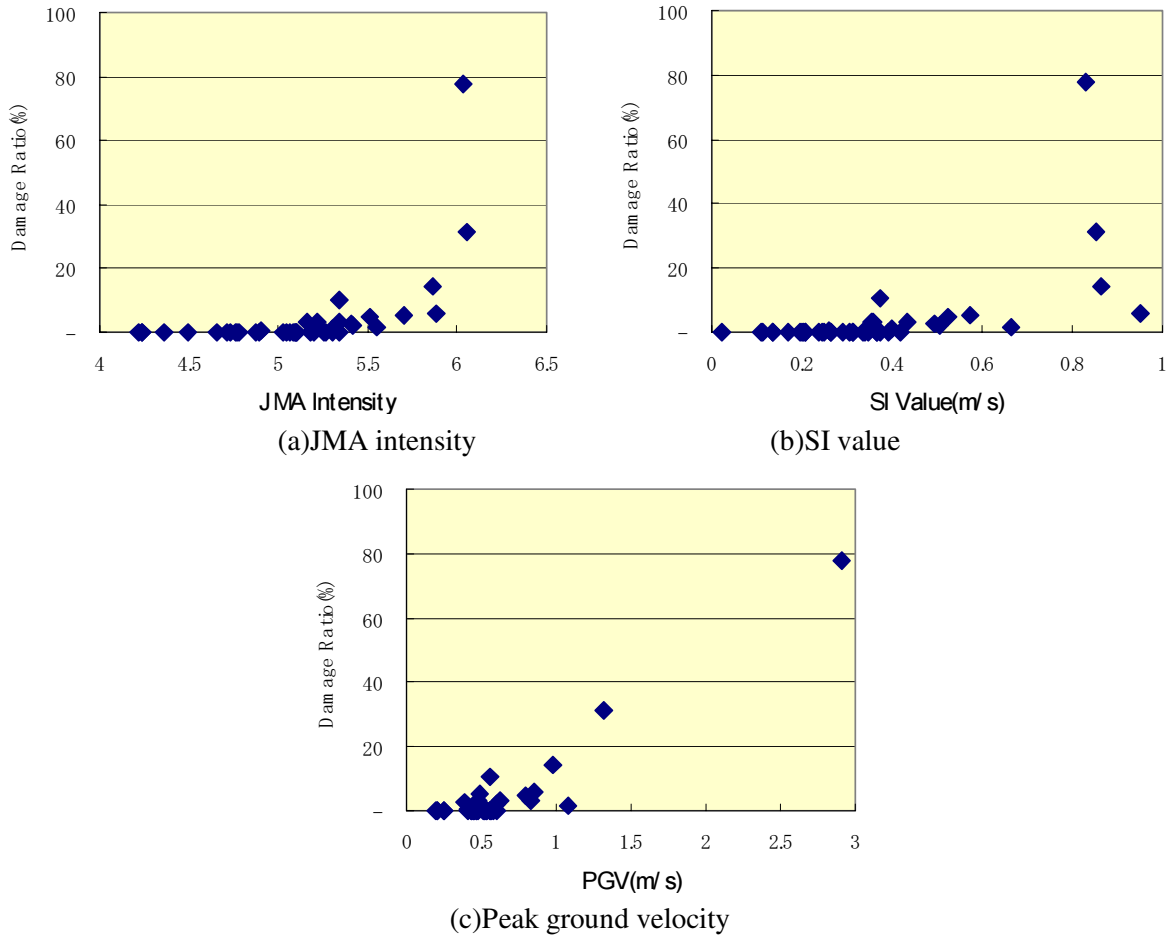


Figure4 Housing collapse rates against the characteristic values

These results can be summarized as follows. The measured seismic intensity and PGV are considered to be appropriate indexes of earthquake damage potential in this case as the long-period motion (>2.5 s) in central Taiwan does not contribute to the calculated SI value. In the fault vicinity, the SI value is small

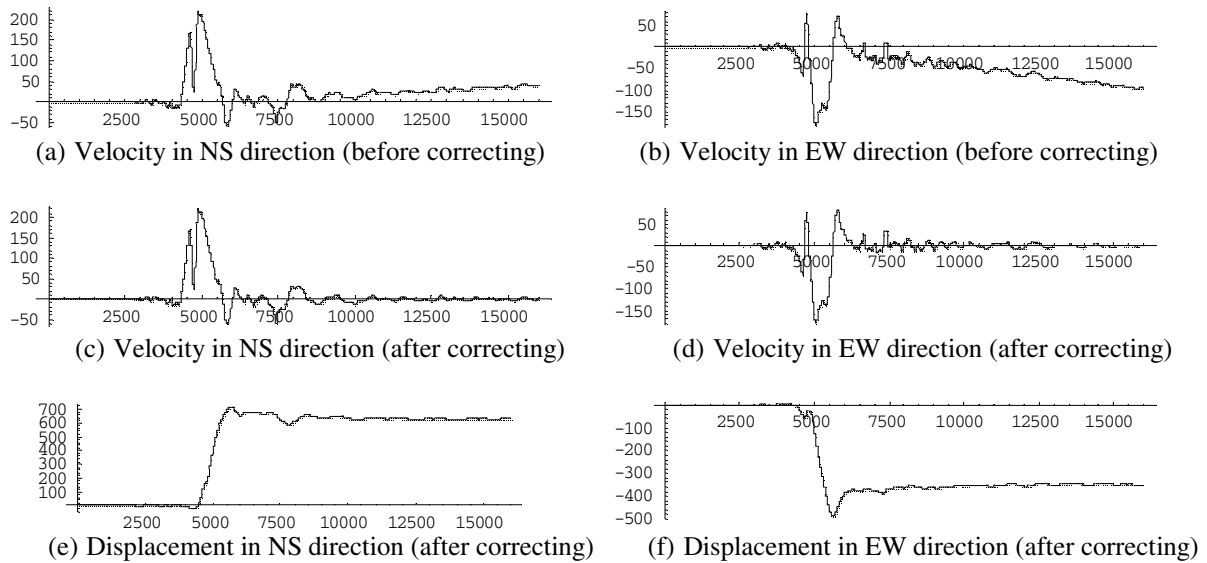


Figure 5 A Calculation Example of permanent Displacement (TCU052)

compared to the seismic intensity or PGV, indicating that care should be taken with the information obtained in this area.

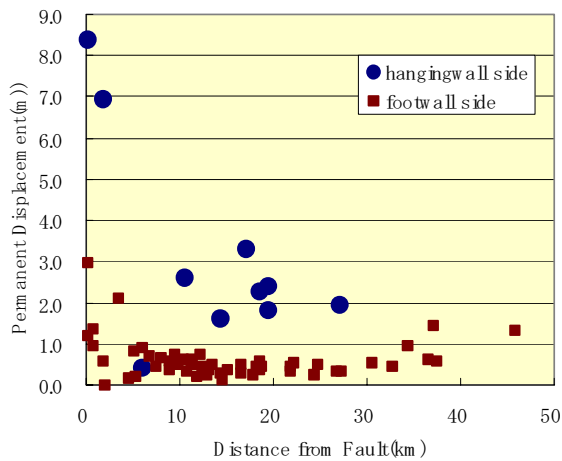
PERMANENT DISPLACEMENT

Calculation of permanent displacement is possible by appropriate noise treatment. The usual method is two-fold integration after band-pass filtering. However, slow movement like the slipping of a fault, is removed by the low-cut filter. Therefore, a better noise reduction method is needed for calculating permanent displacement.

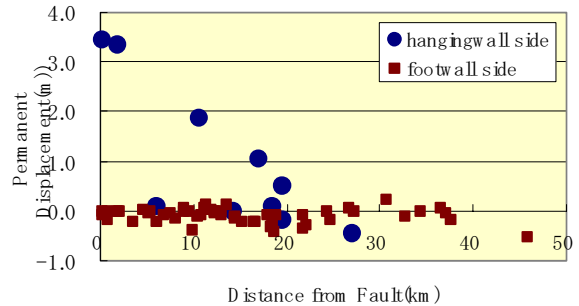
After analyzing the features of the acceleration records in Taiwan, it was noticed that there is a drift in the zero line between the start and end of the motion. D. M. Boore pointed out the tilting of accelerometer (6). This drift reflects tilting of the servo-mechanical accelerometer, with the drift of 17 Gal corresponding to 1° of tilt. Many records exhibit significant drift, particularly TCU084 (9 Gal) and TCU071 (10 Gal). Apparent components like the drift leads to calculation error, and the waveform is effused after integration.

Figures 5(a) and (b) show the results of simple integration of records for the NS and EW components of TCU052 as an example of trapezoidal integration. The horizontal axes of the figures represent the data number, where 10,000 samples corresponds to 50 s, and velocity on the vertical axis is given in cm/s. The drift of the EW component is 0.34 Gal, and 1 Gal for the NS component. The apparent acceleration includes integration error, and therefore deviates after the end of vibration from the velocity zero.

The waveform of the velocity is corrected using the linear regression of the deviating component. The wave data is divided into three parts; pre shock, main shock, and post shock, divided at 3% and 97% of the square sum of the acceleration data. Regression calculation is carried out using the post-shock part, and zero correction is performed for data before the onset of the main shock and after the main shock ends by subtracting the regression trend. This process results in a zero terminal velocity. The integral computation of the corrected velocity data leads to displacement data that includes permanent movement.



(a) Horizontal displacement



(b) Vertical displacement

Figure6 Relationship between the distance from the fault and the permanent displacement

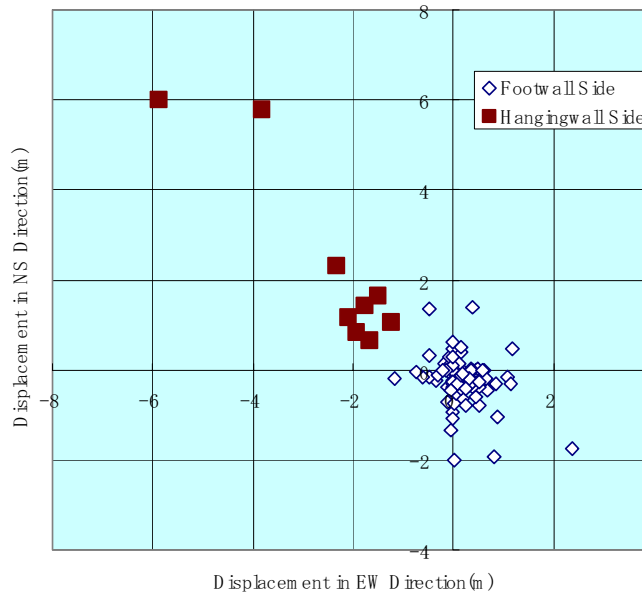


Figure7 Calculated horizontal movement

Figures 5(c) and (d) show the corrected velocity waveform for TCU052. The displacement waveform can then be obtained by a second trapezoidal integration. Figures 5(e) and (f) show the waveforms of displacement in centimeters. The permanent movement is 5–7 m.

A similar calculation was performed for approximately 100 observation points in central Taiwan, although some results could not be obtained due to deviation or corrupted data. Three components of displacement were obtained, and the two horizontal components are combined as an RMS value. The maximum horizontal displacement is 8.4 m, and the maximum vertical displacement is 3.4 m, both occurring at Shrgang.

Figure 6 shows the relationship between the distance from the fault and the permanent displacement. Figure 6(a) shows the horizontal component, and Fig. 6(b) shows the vertical component, with the data distinguished between the hanging wall side and the footwall side. On the hanging wall side, both

horizontal and vertical displacements are attenuated with distance from the fault out to 20 km, whereas the displacement is 1 m or less on the footwall side.

Figure 7 shows the calculated horizontal movement at the observation points. The displacement of points on the hanging wall side is directed toward the northwest, and the vertical displacements are upward. At Puli and Yuchr, located in the mountains, the permanent displacement indicates a slight subsidence. These calculation results are qualitatively consistent with the measurement results announced by the Taiwan land surveying division (7).

CONCLUSION

Housing damage due to the 1999 Chichi earthquake was compared with the observed ground motion in central Taiwan. Index values of PGA, PGV, PGD, SI, JMA intensity, maximum zero cross time, and permanent displacement were calculated from the observed records. The Chichi earthquake occurred in a region deployed with a comprehensive network of seismic monitoring stations, and presents a rare opportunity to analyze ground motion due to a large reverse fault. A long-period pulse with high velocity and large displacement was found to be responsible for the majority of the housing damage. The features learned from the Chichi earthquake, is available for a future earthquake with a reverse fault in estimating damages.

The permanent displacement was calculated by dual trapezoidal integration and elimination of the uncorrected dispersion component. The calculated permanent displacement in central Taiwan including the fault vicinity is consistent with the survey results reported by the Taiwanese government. This analysis demonstrates that it is possible to estimate the permanent displacement from the acceleration records using a suitable algorithm. Therefore, collation of seismic records after an earthquake and calculation of these index values is useful for estimating the characteristics of an earthquake and the extent of damage over a wide area.

REFERENCES

1. Japan Society of Civil Engineers: The Ji-Ji Earthquake, Taiwan –Investigation into damage to civil engineering structures, 1999.
2. W.H.Lee, T.C.Shin, K.M.Kuo, K.C.Chen, and C.F.Wu: Free-Field Strong-Motion Data from the 9-21-1999 ChiChi Earthquake, CWB, 2001
3. T. Suzuki, Y. Shimizu, K. Koganemaru and W. Nakayama: The accuracy of the detection method for liquefaction using zero cross time, Proc. of 26th JCEE, 2001(in Japanese).
4. Tawanese Government: <http://www.kbteq.ascc.net/>.
5. H. Tong and F. Yamazaki: Relationship between the index of strong motion and JMA intensity, IIS report Vo.48,11, pp.547-550, 1996(in Japanese).
6. D.M.Boore:Effect of baseline corrections on response spectra for several recordings of the 1999 Chi-Chi, Taiwan, Earthquake, BSSA, Vol.91-5,2001.
7. Land Survey Bureau in Taiwan: Land survey on catastrophic areas of 921 Earthquake, 2001.